

## Scenario development at JET with the new ITER-like wall

E. Joffrin<sup>1</sup>, M. Baruzzo<sup>2</sup>, M. Beurskens<sup>3</sup>, C. Bourdelle<sup>1</sup>, J. Bucalossi<sup>1</sup>, S. Brezinsek<sup>4</sup>, G. Calabro<sup>5</sup>, C. Challis<sup>3</sup>, M. Clever<sup>4</sup>, J. Coenen<sup>4</sup>, E. Delabie<sup>6</sup>, R. Dux<sup>7</sup>, P. Lomas<sup>3</sup>, E. de la Luna<sup>8</sup>, P. C. de Vries<sup>9</sup>, J. Flanagan<sup>3</sup>, L. Frassinetti<sup>10</sup>, D. Frigione<sup>5</sup>, C. Giroud<sup>3</sup>, M. Groth<sup>11</sup>, N. Hawkes<sup>3</sup>, J. Hobirk<sup>7</sup>, M. Lehnen<sup>4</sup>, G. Maddison<sup>3</sup>, J. Mailloux<sup>3</sup>, C. Maggi<sup>7</sup>, G. Matthews<sup>3</sup>, M. Mayoral<sup>3</sup>, A. Meigs<sup>3</sup>, R. Neu<sup>7</sup>, I. Nunes<sup>12</sup>, T. Puetterich<sup>7</sup>, F. Rimini<sup>3</sup>, M. Sertoli<sup>7</sup>, B. Sieglin<sup>7</sup>, A.C.C. Sips<sup>12</sup>, G. van Roij<sup>9</sup>, I. Voitsekhovitch<sup>3</sup> and JET-EFDA Contributors<sup>\*</sup>

JET-EFDA, Culham Science Centre, Abingdon, OX143PF, UK

<sup>1</sup>IRFM-CEA, Centre de Cadarache, 13108 Sant-Paul-lez-Durance, France.

<sup>2</sup>Associazione Euratom-ENEA sulla fusione, Consorzio RFX, 35127 Padova, Italy

<sup>3</sup>Euratom/CCFE Fusion Association, Culham Science Centre, Abingdon, OX14 3DB, UK.

<sup>4</sup>Association EURATOM/Forschungszentrum Juelich GmbH 52425, Germany

<sup>5</sup>Associazione EURATOM-ENEA sulla Fusione, CNR ENEA Frascati, 00044 Frascati, Italy.

<sup>6</sup>Association EURATOM-Etat Belge, ERM-KMS, Brussels, Belgium

<sup>7</sup>Max-Planck-Institut für Plasmaphysik, Euratom Association, 85748, Garching Germany.

<sup>8</sup>Laboratorio Nacional de Fusion, Asociación EURATOM CIEMAT, Madrid, Spain

<sup>9</sup>Association EURATOM/DIFFER, Rijnhuizen P0 Box 1207 3430BE Nieuwegen, Netherlands

<sup>10</sup>Association EURATOM-VR, Division of plasma physics, KTH, Stockholm, Sweden

<sup>11</sup>Association Euratom-Tekes, Aalto University, Finland.

<sup>12</sup>JET-EFDA-CSU, Culham science site, OX143DB ABINGDON Oxon, UK.

*E-mail contact of main author: [emmanuel.joffrin@cea.fr](mailto:emmanuel.joffrin@cea.fr)*

**Abstract:** In the recent JET experimental campaigns with the new ITER-like-Wall (ILW), major progress has been achieved in the characterisation of the H-mode regime in a metallic first wall: i) plasma breakdown and L-mode operation have been recovered in a few days of operation. ii) Stable type I ELMs H-modes with  $\beta_N \sim 1.4$  have been achieved in low and high triangularity ITER-like shape plasmas and their operational domain at  $H=1$  is significantly reduced with the ILW for equivalent amount of deuterium gas injection than with the carbon wall. iii) Deuterium gas injection ( $10^{22}$ D/s) are needed to control the core radiation. iv) In contrast, the hybrid H-mode scenario has reached H factor close to 1.3 at  $\beta_N$  of 3 for 2 to 3s. iv) In comparison to carbon equivalent discharges, total radiation is similar but the edge radiation is lower and  $Z_{eff}$  of the order of 1.3-1.4. It appears that at low gas fuelling ( $0.5 \cdot 10^{22}$ D/s), impurity transport plays a key role in the behaviour of the H-mode discharges. This paper reviews the major physics and operational achievements and challenges that JET has to face to produce stable plasma scenarios with maximised performance in an ITER-like wall.

### 1. Introduction

The transition to all metal plasma facing components is an essential step on the path to reactor scale fusion devices. The JET ITER-like Wall (ILW) with plasma-facing components (PFCs) made of beryllium in the main chamber and tungsten in the divertor was successfully installed in 2010/11 [1]. Demonstrating the compatibility with the new ILW of typical ITER scenarios such as the baseline or the advanced inductive H-modes (so called “hybrid”) scenarios developed previously in a carbon environment has been one of the main line of the research of the recent JET experimental campaigns.

The paper first presents an overview of the scenario performance and examines its compatibility with the ILW. Then details are given on the H-mode hybrid at high normalised pressure ( $\beta_N \sim 3$ ) and the differences with the H-mode baseline discussed. Plasma composition, tungsten influx and core transport and radiation patterns are important elements to be addressed and compared with the carbon wall in the discussion. Finally the integration of baseline H-mode at high plasma current ( $I_p = 3.5$ MA) is presented. In developing a fully integrated scenario, the main building blocks making a complete discharge from formation to current decay are presented and in particular the current ramp up and down phases, the H-mode termination and the techniques for reducing the impact of disruption.

### 2. Overview of the baseline H-mode development in JET with the ILW

In the JET ILW all the existing Carbon Fibre Composite (CFC) tiles in direct contact with the plasma have been replaced with bulk beryllium as the dominant main chamber material

and with tungsten surfaces in the divertor [1]. The divertor consists of W coated CFC tiles and a single toroidally continuous belt of bulk tungsten at the outer strike point. The anticipated operating limits with the ILW are most fundamentally driven by the relatively low melting point of beryllium (1356C), the limited robustness of tungsten coatings to slow and fast thermal cycles and the thermal capabilities of the support structures for the bulk tungsten tile limiting the energy dumped into the tile row to typically 60MJ without strike point sweeping. The protection of the ILW was an integral part project from very early on and the surface temperature on the tiles (such as the bulk tungsten tile used for the outer strike point) has been systematically monitored [2].

In the initial experimental phases with the ILW, reliable breakdown conditions with pre-magnetisation of the primary current have been recovered in JET in a few discharges and optimised to voltage of the order of that is expected in ITER (~0.25 V.m) [P. de Vries, this conference]. In addition, the interaction with the beryllium (Be) limiter has been minimised using an earlier X-point formation as planned for the early phase of ITER discharges. Early gas fuelling in limiter phase is also essential for developing the discharge in the current ramp-up phase so as to avoid either excessive core radiation or slide-away discharges. L-mode operation with the ILW have shown very low  $Z_{eff}$  (~1.3) plasma, no tungsten accumulation and carbon level down by one order of magnitude with respect to the carbon wall. [3].

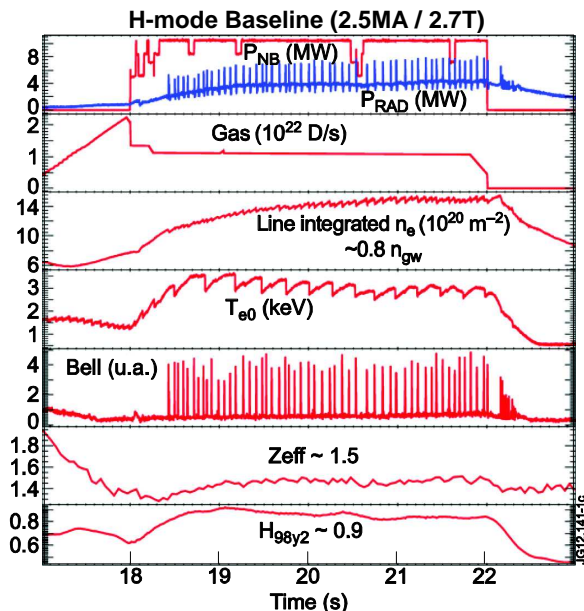


**Fig 1:** typical JET H-mode with the ILW. Note the fuelling rate which is necessary to make the discharge steady.

correlated with strong increase of the bulk radiation and the high Z impurity content (W and Ni), eventually leading to a back transition to L-mode as the power across the separatrix  $P_{LOSS}$  decreases. (here  $P_{LOSS}$  is defined as:  $P_{LOSS}=P_{IN}-dW/dt-P_{RAD,BULK}$ . The last term is the total radiated power inside the last closed flux surface and  $P_{IN}$  the total input power). In this situation, the sawtooth activity does not seem to prevent radiation peaking and even vanishes as the temperature becomes hollow. In general, no disruption occurs if  $P_{IN}$  is maintained, where as switching off the NBI power in such a case can lead to disruption by radiation collapse event.

The increase of the NBI power combined with strong deuterium gas puffing rate (above  $10^{22}$ D/s) opens up the operating space by increasing the ELM frequency and therefore the flushing out tungsten from the bulk plasma. Since both the increase of the loss power and the gas puffing contributes to flush tungsten out by increasing the ELM frequency, it is also found that the minimum gas puffing rate decreases with the loss power.

However, high gas puffing rate has an impact on the confinement of the H-mode (fig 2a). At high triangularity ( $\delta \sim 0.4$ ) the H-mode scenario shows a confinement degradation by 20 to

After this first step, stable Type I H-modes sawtooth regime have been achieved in low and high triangular plasma, at 2.0MA/2.1T and then at 2.5MA/2.7T with  $q_{95} = 3.3$  and neutral beam injection up to ~15MW of input power for 4 to 5s (fig 1). During this initial development phase, impurity events have been observed [J. Coenen, this conference]. In the course of the further operation their frequency remained approximately constant but their effect on plasma less deleterious. It became clear that deuterium had to be puffed at a significant rate (above  $10^{22}$ D/s) in the divertor during the main heating phase to achieve stable conditions in the H-mode regime with respect to central radiation peaking as already shown in ASDEX Upgrade [4]. By scanning the puff rate, a minimum ELM frequency of typically 10 Hz looks necessary to prevent excessive core plasma radiation. Below this limit, long ELM free phases are often

30% with gas puffing which was not observed with the C-wall with similar level of gas fuelling [5]. The low shape case ( $\delta \sim 0.2$ ), cannot be run in the ILW without a minimum gas injection (typically  $10^{22}$  D/s). In the lowest fuelling cases, the confinement factor  $H$  approaches sometimes 1 indicating that the  $H=1$  access is possible but the operating space is reduced with the ILW. In an attempt to open up this space, vertical kicks [6] have been applied to control the ELM frequency. Although the ELM frequency could indeed be controlled at about 20Hz and the gas rate minimised down to  $5 \cdot 10^{21}$  D/s, the confinement factor could not be restored to values closer to 1, hinting to another necessary ingredient responsible for the reduced confinement.

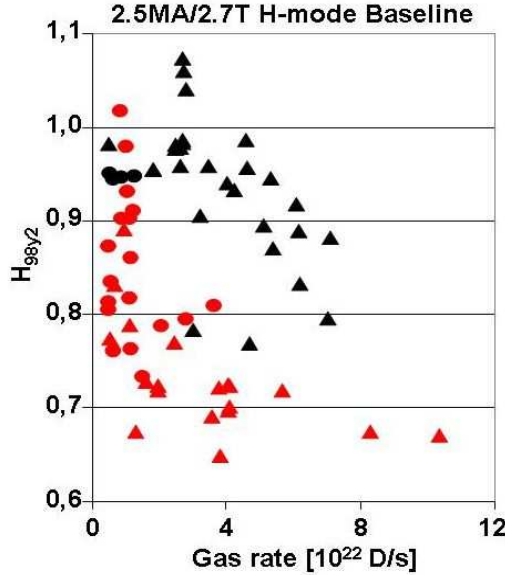


**Figure 2a:** Confinement factor  $H98y2$  function of the gas injection rate for a series of baseline H-mode at 2.5MA/2.7T for both low ( $\delta=0.2$ , circles) and high ( $\delta=0.4$ , triangles) triangularity

The change of the wall composition is most likely at the origin of the difference observed between the C-wall and W-wall.  $Z_{eff}$  is substantially lower with the ILW and a reduction from typically  $\sim 2$  to  $\sim 1.4$  is observed. Bolometric reconstruction shows a significant reduction of the radiated power in the divertor region with the ILW in similar boundary conditions such the edge density. This could play a role in the edge transport barrier and pedestal stability, which would be consistent with first nitrogen seeding experiments with the ILW [7] and AUG results [4] showing an increased edge radiation level comparable to the level observed in the carbon wall.

To understand the relative weight between the source and the tungsten transport in those discharges, radiation profiles have been examined for the H-mode baseline in relation with the tungsten source from the divertor. Figure 2b shows the behaviour of  $P_{radbulk}/\langle n_e \rangle^2$  (representative of the impurity concentration in the discharge) as function of the gas input amplitude. Above 2 to  $3 \cdot 10^{22}$  D/s the level of core radiation is equivalent than with the carbon wall (black points). But this level takes off by dramatically when the gas is lowered. For a selection of these pulses run at same  $I_p$ ,  $B_T$  (2.5MA, 2.7T), same shape and same  $P_{LOSS}$  (from 12 to 14MW), the tungsten source inferred from divertor spectroscopy (photon flux of the 400.8 nm tungsten line) measured over the whole tungsten divertor tile is shown on figure 3. The tungsten decreases with the gas bleed by typically a factor of 2.5 for the low shape and by  $\sim 50\%$  for the high shape, thus much less than  $P_{radbulk}/\langle n_e \rangle^2$  in the same range of gas. Note that these discharges are not in a detached regime according to Langmuir probe measurements. Therefore the separatrix temperature is expected to be well above 5eV. This analysis indicates that the radiation level observed at low gas fuelling is not only caused by the tungsten source, but impurity transport in the core discharge plays a key role in the behaviour of the H-mode discharge.

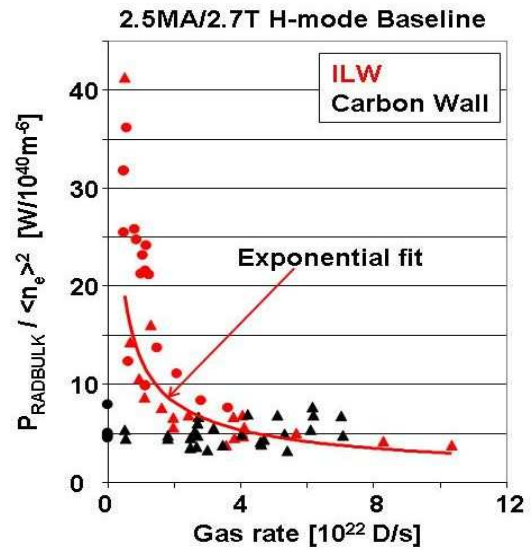


**Figure 2b:**  $P_{radbulk}/\langle n_e \rangle^2$  as function of the gas injection rate for a series of baseline H-mode at 2.5MA/2.7T for both low ( $\delta=0.2$ , circles) and high ( $\delta=0.4$ , triangles) triangularity

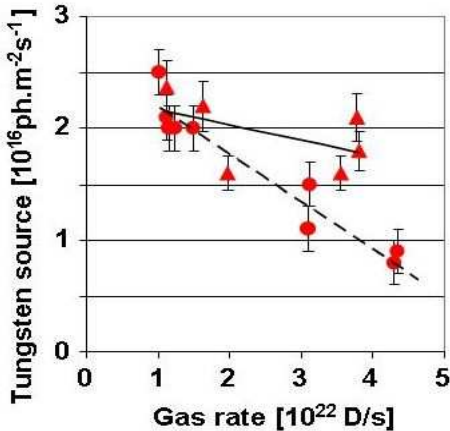


**Figure 3:** Tungsten source integrated over the whole bulk tungsten tile as function of the gas injection rate for both low ( $\delta=0.2$ , circles) and high ( $\delta=0.4$ , triangles) triangularity (using an inverse photon efficiency,  $S/XB \sim 40$ ).

### 3 – The H-mode hybrid scenario up to $\beta_N \sim 3$ and its comparison with the H-mode baseline.

The hybrid scenario has also been developed using as references the work carried out with the C-wall [9], [10]. This scenario is traditionally characterised by its access to high normalised pressure ( $\beta_N > 2.5$ ) and no or infrequent sawteeth activity due to its “broad” q profile shape. The latter is achieved in JET by using the current overshoot technique which helps keeping the central target q value ( $q_0$ ) close to unity and maximising the amount of current density at mid-radius.

For achieving such “non standard” q profiles, the impact of the metallic wall in the current has been first examined experimentally. After the plasma breakdown and an X-point formation 1.4s later, the plasma current is ramped up to its plateau in X-point (as planned for ITER). The comparison with the C-wall shows that more gas had to be injected in this phase to achieve the same plasma density. Too low gas injection (as in the C-wall) resulted in the creation of a run-away electron population (up to 5MeV as detected by  $\gamma$ -ray spectroscopy) and an increased tungsten level which could explain the observed hollow temperature profile in the ramp-up phase. With increased gas injection, the early q profile at the X-point formation is much lower in the plasma core (typically 3 or 4 instead of 6 or 7 as measured by Motional Stark Effect, MSE) than it was with the C-wall in similar conditions. This may have consequences for scenario requiring the control of the target q profile such as the advanced tokamak scenario.

Using this current ramp-up phase, the hybrid scenario has been developed at low shape ( $\delta \sim 0.2-0.3$ ) and high shape ( $\delta \sim 0.4$ ) for  $q_{95} \sim 3.7$  at 1.4-1.7MA/2.0T and 2.0MA/2.3T all using the  $I_p$  overshoot technique (fig 4). In all discharges, the outer strike point was located on the divertor bulk tungsten tile. This was in general not the case with the C-wall where the plasma configuration had a more outward strike point position closer to the pumping louvers of the divertor. Despite the change in plasma shape in the divertor, it appears that the hybrid scenario could reproduce for about 2 to 3s similar global performance ( $H=1.2-1.3$  with  $\beta_N \sim 3$ ) achieved in the C-wall at both high and low triangularity. For the low triangularity, similar H factor than in C-wall is also achieved ( $\sim 1.3$ ) but at higher volume average volume density and lower volume average temperature. In both cases moderate gas fuelling ( $\sim 5 \cdot 10^{21}$  D/s) is required to keep the discharge stable with regard to core radiation. The performance differences observed between the hybrid and the baseline H-modes are not well understood yet, and a detailed comparison is necessary.

Like with the carbon wall, the baseline scenario with the ILW has been operated with a

Bolometric reconstructions for cases of Pradbulk/ $\langle ne \rangle^2$  above  $20\text{MW} \cdot 10^{40} \text{m}^6$  are indeed confirming such central peaking in the low gas fuelled cases. [8].

The neutral recycling is also substantially altered with the ILW as Be/W and C have not the same affinity to deuterium. A higher inter-ELM recycling is observed with the ILW, typically increased by a factor 2 for similar deuterium puffing rate and NBI power conditions while the intra-ELM is strongly reduced. It has to be noted that the deuterium gas puffing rate is still an order of magnitude below the recycling neutral flux but its impact on the confinement appears stronger.

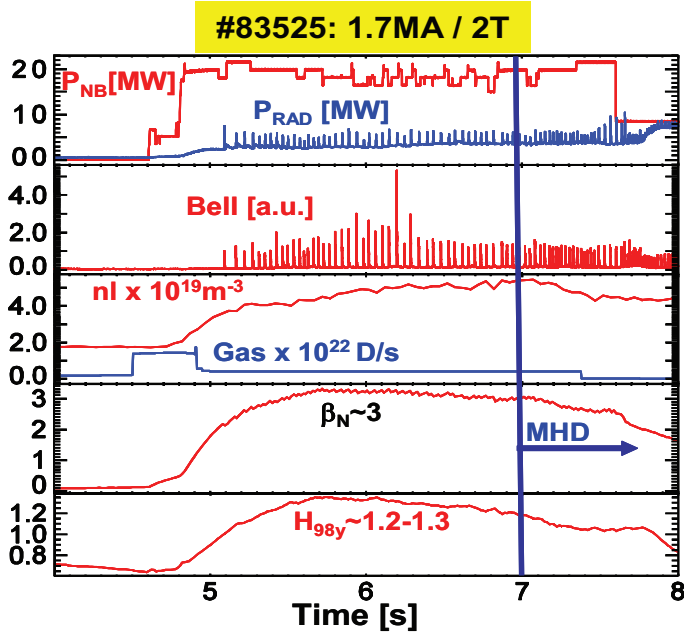


**Fig 4:** Advanced inductive (hybrid) pulse with  $\delta=0.2$  run at JET at  $\beta_N \sim 3$  with the ILW for  $\sim 2$ s. The performances are rolling over when the fishbone activity is replaced by a magnetic island after 7s.

These elements are suggesting that the amount of net power coupled to the H-mode with the ILW is at least equivalent if not higher than with the C-wall.

The baseline and hybrid H-mode scenarios are not run with the same  $I_p$ ,  $B_T$  and  $q_{95}$ . Heating deposition and radiation profiles may be different in these two scenarios. In comparing identical discharges between the C-wall and the ILW, there is no obvious sign that the power deposition and applied torque from the neutral beam injection is significantly different. For the baseline scenario, the radiation profiles from bolometric reconstruction are not showing large differences in the core with respect to the carbon wall unless the gas injection rate is reduced to less than  $10^{22}$ D/s leading to core radiation peaking. In contrast, for the hybrid scenario  $P_{rad,bulk}/\langle n_e \rangle^2$  is in general higher with the ILW by a factor of 2 to 3 even in the case of high (1.2-1.3) H factors.

The understanding of the difference in confinement during the baseline and the hybrid scenarios has also been examined in details looking at the kinetic profiles data [13]. This is done making an extensive use of the high resolution Thomson scattering (HRTS) diagnostic for  $T_e$  and  $n_e$  using a large database (270 pulses) of H-modes baseline and hybrid at both high and low triangularity. In most of the pulses studied the core ion temperature could not be inferred from the charge exchange diagnostics in part because of the low signal over noise ratio resulting from the low carbon concentration with the ILW. However edge/pedestal charge exchange data could be produced and are showing a very similar ion and electron temperature. Therefore at least for the pedestal data, we considered that the observation on electrons also holds for the ions. This analysis shows that the pedestal temperature for the baseline scenario (both low and high shape) is significantly lower (by typically 25 to 30% for an equivalent pedestal density) possibly because of the strong gas fuelling applied to these discharges in general. The hybrid scenario at low shape is also showing low pedestal temperature but also a higher electron density. As a result, the pedestal electron pressure is typically the same between the C-wall and ILW. The hybrid at high shape has also a degraded electron temperature with respect to the C-wall, but this time the density does not seem to compensate entirely for this loss suggesting that the core confinement is improved. From these observations, it seems that the pedestal in the hybrid scenario does not behave in the same way as in the C-wall [13].

The core transport is often characterised by the temperature and density gradient length. Because of the lack of ion temperature measurements, only preliminary conclusions can be

loss power significantly above the power threshold  $P_{th}$  by a factor 1.5 to 2. This indicates that for the baseline scenario, different level of confinement is obtained between the two walls for similar values of  $P_{LOSS}/P_{th}$  at equivalent gas injection rate. The hybrid scenario has also received about the same loss power that with the C-wall, but with much higher level above the threshold, by typically a factor of 2 to 3.5. It should be noted here that the power threshold from Martin's scaling [11] has been derived mostly with data from carbon devices and typically do not account for the radiations. Therefore, it may not represent an appropriate scaling for JET with the ILW. The LH thresholds studies in JET [12] with the ILW are indeed indicating that  $P_{th}$  could be lower than with the C-wall.

drawn from the analysis of  $R/L_T$  and  $R/L_n$  in the core. At high density, the electron-ion equipartition tends to equilibrate the temperature of these two species. This is the case in particular for the high shape plasmas and the high current plasma and this assumption is consistent with the measured thermal stored energy. Looking at the core gradients for this category of discharges, it appears that both  $R/L_T$  and  $R/L_n$  are unchanged for high triangularity baseline scenario. In contrast, the hybrid scenario at high shape shows larger  $R/L_T$  than with the C-wall and similar  $R/L_n$ , consistently with the peaking of density and temperature profiles [13]. This may suggest that for the hybrid high shape scenario there the core transport is lower than with the C-wall and therefore compensates at least partially for the loss of pedestal confinement.

The hybrid scenario with the ILW has in general similar  $m=1/n=1$  continuous activity as in the C-wall. However, the first sawtooth crash can affect the confinement more profoundly (loss of 20% in some cases) [14]. Similarly the  $m=3/n=2$  and  $m=4/n=3$  MHD activity have also been observed, but when an island forms, its effect on the plasma appears to be larger than a simple flattening of electron temperature profile within the island, but showing indeed a slow decrease of central electron temperature and an enhanced radiation from the plasma core (as observed on the increased soft X-ray level). This is in contrast to observations with the C-wall where such events could be recovered from and did not terminate the discharge in radiative collapse. In ILW discharges,  $\beta$  control by the NBI power is used. More stable operation could be successfully achieved by setting up a lower  $\beta$  target (2.7 instead of 3.0), but with a performance penalty ( $H \sim 1.1-1.2$  instead of 1.3). The internal MHD signature of the H-modes can play a significant role between the hybrid and baseline H-modes on the transport of impurity towards the core plasma. The sawtooth and the tearing modes could change dramatically the particle transport properties in the hybrid H-mode and lead to radiative collapse. In the baseline H-mode sawtooth phases seem to be responsible for the long term evolution of central accumulation leading to radiation instabilities [8]. The role of sawteeth in the inward and outward transport of high Z impurities [15] will therefore require specific investigations in ILW plasmas.

#### 4. H-mode baseline scenario at $I_p=3.5\text{MA}$ and its integration in the ILW.

On the basis of the first H-mode regime developments at  $2.5\text{MA}/2.7\text{T}$  ( $q_{95}=3.5$ ), low triangularity ( $\delta=0.2$ ) baseline operational domain has been extended up to  $3.5\text{MA}/3.2\text{T}$  ( $q_{95} \sim 3$ ). This provides a domain to lower  $\rho^*$  and  $v^*$  and thus interesting data for the study of ELM heat load, density peaking and confinement scaling as it was done with the C-wall [16]. Large gas injection has been intentionally used again to stabilise the discharge and keep the ELM frequency above  $\sim 10$  to  $20\text{Hz}$  and strike point sweeping of about  $\pm 6\text{cm}$  has been successfully applied at the bulk tungsten tile to mitigate the surface temperature tile below  $1200\text{C}$ . Using this cautious approach, plasmas have been successfully developed at  $\beta_N \sim 1.4$  with  $25\text{MW}$  of NBI power for more than  $5\text{s}$  duration and a  $Z_{\text{eff}}$  of  $1.2-1.3$  (fig 5). ICRH power has also been coupled successfully up to a level of  $3.5\text{MW}$ . An elevation of the core temperature and larger sawtooth activity are clearly observed in the ICRH phase but there is no clear evidence yet that it had a beneficial effect on the high Z impurity core concentration. In comparison to the C-wall high current scan with the same triangularity, the confinement is consistently lower by 20 to 30% at same plasma current,  $q_{95}$  and shape. This has been achieved despite injecting 50% more power than the power threshold  $P_{\text{th}}$  from the ITPA Scaling [11], which is equivalent to what had been done with the C-wall. Attempts to recover the confinement by lowering the gas injection down to a rate of  $2 \cdot 10^{22} \text{ D/s}$  and increasing  $P_{\text{LOSS}}/P_{\text{th}}$  well above 2 while keeping the ELM frequency above  $10\text{Hz}$ , have not succeeded in recovering more than 10% of the confinement. As a result, the  $\rho^*$  and  $v^*$  range are higher by typically 50% and 30% respectively than with the C-wall.

For the baseline scenario at  $3.5\text{MA}$ , an absolute force of  $600\text{T}$  could be expected in case of a vertical displacement event. To mitigate such event, the massive gas injection (MGI) has been used routinely in closed loop above plasma currents of  $2.5\text{MA}$ . With the ILW, lower radiation is observed during the disruption resulting in a higher fraction of the magnetic energy to be conducted, thus higher heat loads on the wall. In addition, the longer current quench is also

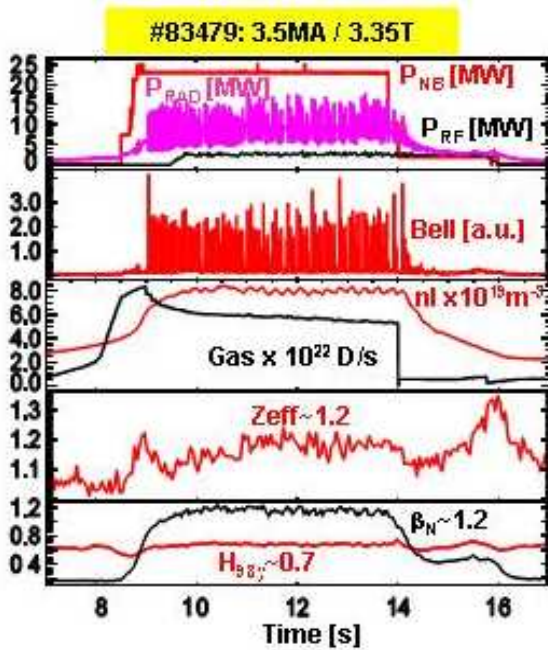


**Fig 5:** 3.5MA pulse run at JET with the ILW. Note the strong D gas puffing rate and the plasma termination using a tail of ICRH and NBI power for 2s.

radiation distribution towards more plasma core radiation, switching off the power at termination often resulted in a radiative collapse. This may be explained by the longer residence time of heavy impurities in the plasma than that of light impurities. The use of electron heating up to (4MW of ICRH) in the landing phase has been successful in mastering the landing of the HL transition. In this phase, the electron temperature could be increased up to 6 or 7keV and helped in preventing radiation collapse. However more dedicated experimental work is necessary to understand the physics processes associated with the back-transition and the external transport barrier collapse.

In addition, dedicated experiments have been carried out to investigate the H-mode in the ramp-up and ramp-down phase. The goal is to address the flux consumption and the internal inductance ( $l_i$ ) evolution in these phases in the ILW environment and assess whether these phases could be limited by the poloidal field system of ITER as it was done with the carbon wall [21], [22]. In this type of experiment the current ramps are scaled to ITER using the resistive time ( $\sim \langle T_e \rangle^{3/2} \cdot a^2$  at fixed  $Z_{eff}$ ) as a guide, resulting in current ramp-up rates of typically 0.36 to 0.28MA/s. The range of internal inductances achieved in ohmic and H-mode at the end of the current rise is comparable to that obtained with the C-wall. Furthermore, in H-mode, the flux consumption in the current rise is less than in the C-wall by typically 25%. The current ramp-down has been investigated along the same guide lines for ramps of -0.14 to -0.5MA/s. Although  $l_i$  increases from 0.9 to 1.2 in H-mode, the increase is limited as long as the discharge stays in H-mode like. These results are in line with those obtained with the C-wall and therefore confirm that there even for the fastest ramp-down it is possible to maintain plasma vertical position and avoid any significant flux consumption in the ramp-down of ITER. In general no increase of the core radiation is observed in these experiments.

ITER-like ramp-up and down, disruption mitigation and H-mode termination studies are essential and paving the way to the demonstration baseline discharges in an ITER-like metallic environment.

## 5. Conclusions

The recent experiments at JET with the new ILW have made significant progress in the scenario integration with a relevant wall for ITER. Stable H-mode baseline plasma ( $q_{95} \sim 3$ ,  $\beta_N \sim 1.4$ ) have been achieved in JET for about 5s up to a current of 3.5MA with a confinement

producing higher halo forces [17]. The experiments to qualify the efficiency of the DMV on disruption have shown that [18], the MGI increases the radiation and thus reduces the heat loads and forces. To trigger the MGI, a set of sensors have been used routinely based on the lock-mode signal and current quench detectors (detecting  $dI_p/dt$  or poloidal flux variations) [19]. These trigger acted more than 67 times for current of 2.5MA and above. In addition, a more sophisticated real time predictor based on a combination of classifier of 7 characteristic temporal signals has been designed [20] and tested off-line. It demonstrated that with the ILW almost 90% of the disruptions can be predicted 30ms in advance of the disruption, with thus a success rate higher than the single signal based detectors.

The scenario development at high current have also been investing significant amount of time in mastering the H mode termination and landing. Because the ILW has changed the

factor  $H_{98y2}$  in the range of 0.7-0.9. Hybrid H-modes above  $\beta_N=3$  at  $I_p=2MA$  ( $q_{95}\sim 4$ ,  $\beta_N\sim 3$ ) with and  $H_{98y2}$  factor exceeding 1.2 for 2s. Although operational issues such as the limited steady state heat load or the changes in plasma impurity composition were foreseen, the landscape of scenario operational domain has changed more significantly than expected, but is consistent with the observation on other metallic devices such as ASDEX Upgrade [4] or C-MOD [23]. The most important results is that the access to  $H\sim 1$  confinement is in general much more restricted than with the carbon wall for the baseline H-mode scenario in both low ( $\delta=0.2$ ) and high shape ( $\delta=0.4$ ). The need to control core radiation with significant gas puffing rate (above  $\sim 10^{22}D/s$ ) plays a major role in this result. In particular, the access to a confinement factor of  $H=1$  is seriously restricted because of the need to use gas injection to lower the tungsten source and increase the W transport. Although the W contamination can be clearly observed as function of gas fuelling and PLOSS, the evidence is pointing towards the key role played by the high Z impurity transport. The lower  $Z_{eff}$  ( $\sim 1.3$ ) and lower radiation (and higher separatrix temperature) in the divertor in comparison to the carbon wall could also play a key role in the scrape off layer transport. The observation that part of the stored energy in the baseline H-mode can be recovered using nitrogen injection [7] is a signature that the link between the SOL and the core confinement does exist.

However, even with some gas injection ( $\sim 510^{21}e/s$ ), H factor close to 1.3 can be reached in the hybrid H-mode scenario in JET with the ILW. At this point, it is not yet clear why in contrast to the baseline H-mode, the hybrid H-mode achieves the similar H factor than with the C-wall. The observation are suggesting that the changes of both pedestal and core kinetic profiles are not identical between the two scenarios. The higher  $q_{95}$  ( $\sim 4$ ) and the level of plasma current ( $<2MA$ ) so far used in the hybrid scenario could be beneficial. Future experiments aiming at developing the hybrid H-mode to higher current and therefore higher thermal and particle confinement time and longer duration could shed more light on the observed differences. It should also be noted that the MHD stability in these discharges has become a critical issue for the future because of its consequence on the impurity transport. In addition, the ILW has motivated the integration of key elements such as the use of the MGI, the landing of the H-mode and the study of the current ramp-up and –down. This integration work remains essential in the development of the scenario in preparation for ITER.

## 6. References

- [1]: G. Matthews et al. 20th PSI Conference, Aachen, Germany, 2012, to be published in JNM.
- [2]: G. Arnoux et al. HTPD Conference, Monterey, CA, USA, 2012.
- [3]: S. Brezinsek et al., this conference
- [4]: R. Neu et al., 20th PSI Conference, Aachen, Germany, 2012, to be published in JNM.
- [5]: G. Saibene et al., Nuc. Fus. 39, (1999) 1133
- [6]: E. de la Luna et al., , this conference
- [7]: C. Giroud, this conference
- [8]: T. Puetterich et al., this conference
- [9]: J. Hobirk, et al. PPCF 54 095001
- [10]: E. Joffrin et al., 2010 FEC conference, Daejeon, Korea, EXC/1-1
- [11]: Y. Martin et al., (2008), J. Phys. Conf. Ser. 123012033
- [12]: C. Maggi et al. 39<sup>th</sup> EPS Conference, 03-108, Stockholm 2012
- [13]: M. Beurskens et al., this conference
- [14] : M. Baruzzo et al., 54th APS annual meeting, Providence, RI, USA,2012.
- [15] : F. Nave, et al., Nucl. Fusion 43 (2003) 1204
- [16]: I. Nunes et al., 2010 FEC conference, Daejeon, Korea, EXC/P8-03
- [17]: P. de Vries et al., 39<sup>th</sup> EPS Conference, Stockholm 2012, to be published in PPCF
- [18] : M. Lehnen et al., this conference
- [19]: C. Reux et al 27th SOFT conference, Liege, Belgium
- [20] : J. Vega et al., 27th SOFT conference, Liege, Belgium
- [21]: A.C.C. Sips et al., Nuc. Fus. 2009
- [22]: I. Nunes et al., 38th EPS Conference, P4-106, Strasbourg, 2011
- [23]: E. Marmar et al., Nuc. Fus 49 104014

---

\* See the Appendix of F. Romanelli et al., Proceedings of the 24nd IAEA Fusion Energy Conference 2012, San Diego, USA.